

Learning from Synthetic Data for Visual Grounding

Ruozhen He¹ Ziyan Yang¹ Paola Cascante-Bonilla² Alexander C. Berg³ Vicente Ordonez¹
¹Rice University ²University of Maryland ³University of California, Irvine

Abstract

This paper extensively investigates the effectiveness of synthetic training data to improve the capabilities of vision-and-language models for grounding textual descriptions to image regions. We explore various strategies to best generate image-text pairs and image-text-box triplets using a series of pretrained models under different settings and varying degrees of reliance on real data. Through comparative analyses with synthetic, real, and web-crawled data, we identify factors that contribute to performance differences, and propose SynGround, an effective pipeline for generating useful synthetic data for visual grounding. Our findings show that SynGround can improve the localization capabilities of off-the-shelf vision-and-language models and offers the potential for arbitrarily large scale data generation. Particularly, data generated with SynGround improves the pointing game accuracy of a pretrained ALBEF and BLIP models by 4.81% and 17.11% absolute percentage points, respectively, across the RefCOCO+ and the Flickr30k benchmarks.

1. Introduction

Vision-and-language models pretrained on large-scale image and text pairs have become exceedingly accurate across various tasks [6, 33, 41, 44, 45, 49, 51, 59, 64]. By leveraging web-sourced datasets, these models showcase a strong ability to comprehend and process an extensive vocabulary of objects and scenes, demonstrating remarkable performance. Our work focuses on the task of visual grounding, which consists of mapping arbitrary input text to image regions. Recent methods finetune vision-and-language models pretrained on web-scale image-text pairs with a large but more modest number of images annotated with bounding boxes or other region annotations; alternatively, these methods leverage pretrained object detectors that have been trained on such annotated data [11, 12, 21, 27, 34, 35, 45, 92, 94]. The resulting vision-and-language models can then be used to perform visual grounding over an arbitrary vocabulary of objects.

Collecting annotations for tasks that require localizing

objects is considerably more expensive than for other tasks. Region annotations in the form of bounding boxes or segments can not be easily obtained from the web in the same way that image-text pairs can be found, and require more cognitive effort to annotate manually than providing a single label. For instance, curating the widely used Visual Genome [39] dataset involved contributions from 33,000 unique workers over 6 months, following 15 months of experimentation and refinement of the data representation. The massive manual demand restricts the scale of such region-annotated data compared to the image-text datasets at the billion scale [76]. Recent work has championed the use of synthetic data – *learning from models* – even for tasks that require only image-text pair supervision [81]. Our work takes this paradigm one step further by investigating whether synthetic data obtained from models is ready to make significant improvements for the visual grounding task, where we need to obtain high-quality samples in the form of image-text-region triplets.

In this paper, we take advantage of recent advancements in text-to-image generation [56, 68, 74], large language models [13, 83] and models for other vision-and-language tasks [43, 45, 48] to design an effective pipeline to supervise vision-and-language models for visual grounding. We refer to this pipeline as *SynGround* and present a systematic analysis to justify each stage of our data generation process. While there have been several attempts in training visual recognition models with synthetic data by leveraging automatically generated image-text pairs [4, 23, 29, 75, 81, 82], our work is the first to also leverage generative models for synthesizing grounded image data. Moreover, we assess the efficacy of synthetic data by comparing it to real and web-crawled data, identifying specific factors that limit its performance. We also investigate whether synthetic data can augment real data and examine its scalability.

Our key findings and contributions are summarized as follows: (1) For a text-to-image generative model, detailed prompts obtained from image captioners yield the most effective synthetic image-text pairs for visual grounding, surpassing those generated from concatenated region descriptions or LLM-generated text. (2) To obtain synthetic image-text-boxes, both layout-conditioned genera-

tive models and object detectors using synthetic image-text pairs show promise. However, layout-conditioned models are more limited. (3) We use our findings to propose SynGround, an effective pipeline to synthesize image-text-boxes for visual grounding. This method leverages exhaustive image descriptions for image synthesis, an LLM for text synthesis from phrase extraction, and an open-vocabulary object detector for bounding box generation. (4) Our results show that using our generated synthetic data outperforms using web-crawled data (Sec. 5.5). Additionally, our synthetic data can effectively augment real data (Sec. 3.3) and shows an upward trend in terms of scalability (Sec. 5.4).

2. Related Work

Visual Grounding. Visual grounding associates textual descriptions with relevant regions within images. Supervised methods are typically trained with image-text-box pairs [17, 18, 21, 35, 94], or integrate pretrained object detectors [28, 66] to identify the most relevant regions with respect to textual descriptions [11, 15, 25, 27, 50, 87]. While weakly-supervised methods bypass the need for bounding boxes [3, 30, 78, 79], they rely on datasets such as Visual Genome [39], which provides multiple phrases describing various regions in each image. However, the process of manually annotating dense textual descriptions and their corresponding boxes is time-consuming. Although some studies collect more data [90] or generate annotations for existing image-text datasets [62, 89, 96], we posit that our contribution is orthogonal as we aim to investigate the feasibility and limitations of generating and using synthetic data. Related to grounding methods incorporating tuning of visual explanations [30, 41, 91, 94], we explore visual grounding in a more general context, aiming to localize phrases using gradient-based model explanations (i.e. Grad-CAM [77]) rather than generating boxes [45]. Compared to boxes, explanation maps provide a more flexible representation that can be used for text referring to multiple objects or background regions. The state-of-the-art grounding method in this category is AMC [94], which proposed an attention mask consistency objective to optimize the gradient-based explanations of ALBEF [41] to improve localization performance. We adopt ALBEF as our main base model and tune it with attention mask consistency on image-text-box triplets as a testbed for our generated data.

Learning from Synthetic Data. The use of synthetic data has been widely explored across various computer vision tasks, including image classification [24, 54, 61], semantic segmentation [10, 67, 69], object detection [60, 72], human pose estimation [37, 85], action recognition [86], and many other domains [1, 14, 31, 40, 52, 53, 55, 70, 71, 84, 93, 95]. In contrast to works that generate synthetic data using 3D-rendering [26, 98] or physically realistic engines [7, 8, 16, 20, 24], our approach aligns more closely

with research adopting diffusion models. He *et al.* [29] use GLIDE [56] for generating synthetic images to improve a pretrained CLIP model [64] in zero-shot and few-shot classification, while its performance is adversely affected when trained from scratch on synthetic data. Azizi *et al.* [4] fine-tune Imagen [74] on ImageNet [73] and subsequently leverage its synthetic data to augment the real ImageNet training set, resulting in initial improvement followed by degradation upon scaling up. Fan *et al.* [23] investigate the scaling laws of synthetic images and identify related factors. StableRep [82] propose a self-supervised method with a multi-positive contrastive loss that learns representations from synthetic images generated for captions in large-scale datasets [9, 19], thereby boosting linear probing image classification performance. SynCLR [81] uses LLM-generated synthetic captions. Our research not only generates image-text pairs but also provides corresponding synthetic boxes, facilitating a comprehensive exploration of the efficacy of synthetic image-text-box triplets in visual grounding.

3. Methodology

We investigate effective strategies to generate image-text-boxes $\langle I, T, B \rangle$ to improve the visual grounding ability of a generic vision-and-language model. This model comprises a text encoder ϕ_t , a visual encoder ϕ_v , and a multimodal fusion encoder ϕ_f . We first introduce the objectives for tuning the base model on image-text pairs $\langle I, T \rangle$ and image-text-box triplets $\langle I, T, B \rangle$. Sec. 3.1 explores various image-text synthesis strategies with an image generator Ψ_g , while Sec. 3.2 delves into multiple approaches for box synthesis. In the following sections, we conduct extensive experiments and analyses with our proposed image-text-box synthesis, SynGround, which integrates an image caption generator Ψ_c , a text-to-image generator Ψ_g , a large language model Ψ_t and an object detector Ψ_d . Sec. 3.3 shows evaluation of SynGround when combined with Real Data.

Preliminaries and Setup

Image-Text Matching. We adopt ALBEF [41] as the main base model which incorporates image-text matching objectives including a standard image-text matching loss (\mathcal{L}_{itm}), an image-text contrastive loss (\mathcal{L}_{itc}) and a masking language modeling loss (\mathcal{L}_{mlm}). The image-text matching loss \mathcal{L}_{itm} evaluates the compatibility between an image and a text by analyzing the output of [CLS] tokens. This loss measures how well a given image-text pair $\langle I, T \rangle$ matches using a cross-entropy loss. The image-text contrastive loss \mathcal{L}_{itc} is designed to align visual and textual representations using contrastive learning by sampling a set of negative samples and a temperature scaling parameter to normalize the scores. The masking language modeling loss \mathcal{L}_{mlm} uses both visual inputs and textual context to predict masked tokens from the input text. The overall objective to tune the

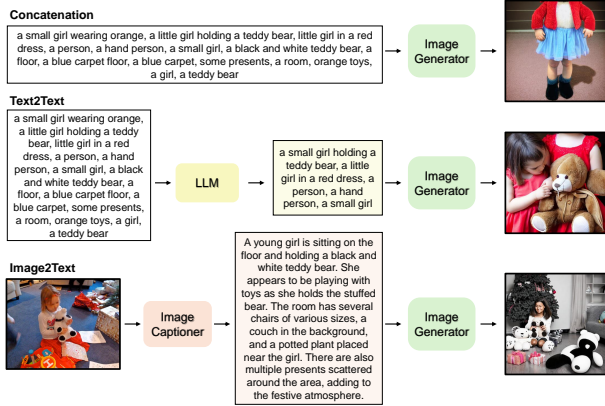


Figure 1. Various approaches for obtaining text descriptions to use as input prompts for an image generator, resulting in image-text pairs. 1) **Concatenation**: Descriptions are generated by concatenating real text, 2) **Text2Text**: LLM summary on real text, and 3) **Image2Text**: Descriptions are produced from an image captioner.

base model on image-text pairs is $\mathcal{L}_{v1} = \mathcal{L}_{itm} + \mathcal{L}_{itc} + \mathcal{L}_{mlm}$.

Image-Text-Box Matching. We adopt an attention mask consistency objective \mathcal{L}_{amc} to add region-level box supervision on top of the ALBEF model [94]. This objective uses gradient-based explanation heatmaps G through Grad-CAM [77], and maximizes the consistency between this map and region annotations. This objective considers two terms. The first term \mathcal{L}_{max} encourages the maximum value of G inside a target box B to surpass the maximum value outside by a margin δ_1 .

$$\mathcal{L}_{max} = \mathbb{E}_{(I,T,B) \sim D} \left[\max(0, \max_{i,j}((1 - B_{i,j}) G_{i,j}) - \max_{i,j} (B_{i,j} G_{i,j}) + \delta_1) \right],$$

where $B_{i,j}$ is 1 when pixel location i, j is inside the box, and zero otherwise. The second term \mathcal{L}_{mean} encourages the mean value of heatmap G inside the box to be larger than the mean value outside by a margin δ_2 .

$$\mathcal{L}_{mean} = \mathbb{E}_{(I,T,B) \sim D} \left[\max(0, \frac{\sum_{i,j} (1 - B_{i,j}) G_{i,j}}{\sum_{i,j} (1 - B_{i,j})} - \frac{\sum_{i,j} B_{i,j} G_{i,j}}{\sum_{i,j} B_{i,j}} + \delta_2) \right].$$

The full \mathcal{L}_{amc} objective is $\mathcal{L}_{amc} = \mathcal{L}_{max} + \lambda \cdot \mathcal{L}_{mean}$, where λ is a trade-off hyperparameter. The base model is tuned with both \mathcal{L}_{v1} and \mathcal{L}_{amc} on image-text-box triplets.

Visual Grounding Evaluation. Following prior works for Visual Grounding methods that predict heatmaps, our evaluation uses pointing game accuracy, which measures the proportion of instances where the maximal activation point within generated heatmaps correctly falls within the annotated ground-truth box regions [2, 15, 21, 27, 30, 41, 50, 94]. We conduct evaluation across multiple benchmarks, including RefCOCO+ [97] and Flickr30k [63].

3.1. Generating Synthetic Image-Text Pairs

To generate image-text-box triplets for visual grounding, we first explore synthesizing effective image-text pairs for visual grounding. As illustrated in Fig. 1, we investigate three alternatives for conditioning a text-to-image generation model Ψ_g . (1) **Concatenation**: merging all captions of a real image I as a prompt for Ψ_g . (2) **Text2Text**: Using an LLM Ψ_t to create a cohesive prompt given a set of text descriptions. (3) **Image2Text**: Employing an image captioning model Ψ_c to generate new captions for real images I^R as prompts for Ψ_g . Table 1 compares these strategies. We tune all of the models in these experiments using the image-text matching objectives \mathcal{L}_{v1} . Although image-text matching objectives are not designed specifically for visual grounding, well-aligned region phrases from Visual Genome (VG) can improve visual grounding performance by 0.96% on average (row 2).

The **Concatenation** strategy (Syn-C) degrades the average performance by 1.60%, indicating that the text-to-image generation model Ψ_g is ineffective with long yet potentially redundant prompts. For **Text2Text**, LLM summaries generated synthetic image (Syn-V) show misalignment with the original VG captions (row 4). Also, tuning the model on Syn-V and object-centric phrases obtained by splitting the LLM summary with commas (LLM_C) is ineffective (row 5). For the **Image2Text** strategy, we experiment with two distinct styles of image captioning models: BLIP-2 [43] that yields condensed phrases, and LLaVA [48] that produces detailed paragraphs. Both BLIP-2 and LLaVA prompted images (Syn-B and Syn-L, respectively) show partial overlap with real VG captions (rows 6 and 8). Notably, an opposite influence is observed when Syn-B and Syn-L are paired with phrases extracted from their captions. BLIP-2 captions, usually short and object-centric (e.g., “a dog, a cat”), are split into phrases by commas, showing improved performance over Syn-B and VG captions, possibly due to better cross-modal alignment, but still below the baseline.

We find that LLaVA-synthesized images (Syn-L) paired with phrases extracted from LLaVA captions can enhance grounding performance (Table 1, rows 11 and 12). This indicates that detailed prompts suit the text-to-image synthesis model better. We compare four ways to partition the LLaVA captions into phrases: LLaVA_P and LLaVA_C, segmented by periods and commas, respectively, LLaVA_L for longer LLM extracted phrases and LLaVA_S for shorter phrases. Our experiments demonstrate that the **Image2Text** strategy, particularly with LLaVA captioning and LLM phrase extraction, yields the most effective synthetic image-text pairs for visual grounding. *More details in the supp.*

3.2. Generating Synthetic Image-Text-Box Triplets

This section discusses two pipelines for image-text-box synthesis. The first pipeline builds on the success of *Im-*

Table 1. Comparisons of image-text synthesis strategies. We assess the effectiveness of synthetic image-text pairs from text concatenation, Text2Text, and Image2Text pipelines, by evaluating the performance improvements over an ALBEF model. For reference we also include the performance that would be obtained by finetuning ALBEF on real image-text pairs from Visual Genome (VG).

Category	Row	Image	Text	$\langle I, T \rangle$	RefCOCO+		Flickr30k	Δ_{avg}
					Test A	Test B		
ALBEF	1	-	-	-	69.35	53.77	79.38	-
ALBEF + VG	2	VG	VG	1,649,546	71.41	54.06	79.90	+0.96
Concatenation	3	Syn-C	VG	1,649,546	67.57	53.14	76.99	-1.60
Text2Text	4	Syn-V	VG	1,649,546	67.41	52.14	77.80	-1.72
	5	Syn-V	LLM _C	530,233	70.28	52.08	78.97	-0.39
Image2Text	6	Syn-B	VG	1,649,546	56.88	48.48	73.93	-7.74
	7	Syn-B	BLIP-2 _C	267,199	68.15	51.50	78.30	-1.52
	8	Syn-L	VG	1,649,546	65.35	50.28	76.85	-3.34
	9	Syn-L	LLaVA _P	384,455	70.22	52.30	78.34	-0.55
	10	Syn-L	LLaVA _C	716,198	69.94	53.26	78.83	-0.16
	11	Syn-L	LLaVA _L	680,093	69.84	53.61	79.44	+0.13
	12	Syn-L	LLaVA _S	1,031,521	70.31	52.55	80.73	+0.36

Table 2. Efficacy of synthetic image-text-boxes generated with either GLIP [45] or GLIGEN [46]. For reference, we also include the reported performance of finetuning ALBEF [41] with an AMC loss [94] on real image-text-box triplets from Visual Genome (VG).

Model	Row	Image	Text	Box	$\langle I, T, B \rangle$	RefCOCO+		Flickr30k	Δ_{avg}
						Test A	Test B		
ALBEF	1	-	-	-	-	69.35	53.77	79.38	-
AMC	2	VG	VG	VG	1,649,546	78.89	61.16	86.46	+8.00
ALBEF	3	Syn-A	VG	VG	1,649,546	68.79	56.88	84.57	+2.58
	4	Syn-R	VG	VG	1,649,546	68.25	55.78	84.59	+2.04
+	5	Syn-R	VG _R	VG _R	725,974	71.66	56.15	84.84	+3.38
GLIGEN	6	Syn-T	VG _T	VG _T	725,974	71.80	56.68	84.73	+3.57
	7	Syn-I	VG _I	VG _I	652,657	73.05	58.38	84.39	+4.44
ALBEF	8	Syn-L	LLaVA _L	GLIP	659,927	72.39	55.94	86.53	+4.12
+	9	Syn-L	LLaVA _{S,L}	GLIP	1,658,333	72.25	57.05	86.71	+4.50
GLIP	10	Syn-L	LLaVA _S	GLIP	998,406	73.70	56.35	86.89	+4.81

age2Text (Sec. 3.1) and additionally uses an open vocabulary object detector Ψ_d [45] to generate region annotations for each synthetic text phrase. Fig. 2 shows an overview of this strategy. As shown in Table 2, we compare pairing synthetic images with shorter phrases (LLaVA_S), longer phrases (LLaVA_L), and both (LLaVA_{S,L}). The shorter phrases outperform others (row 10), leading to an average performance gain of 4.81%. However, combining shorter and longer phrases (LLaVA_{S,L}) –despite increasing the amount of data– does not further improve performance, suggesting redundancy in the information conveyed by phrases with different lengths.

We also investigate an alternative strategy that leverages

a layout-conditioned generative model GLIGEN [46], synthesizing images conditioned on the text and corresponding bounding boxes. Directly inputting all real VG texts and boxes (row 3) results in a modest increase of 2.58% compared to the baseline (row 1). We observe the ineffectiveness of using regions with multiple textual descriptions, as this tends to generate unrealistic or implausible content. To address this, we explore three strategies: Random selection of text-box inputs (VG_R), reduction based on average CLIP [64] text dissimilarity (VG_T), and selecting the maximum number of boxes with an IoU below 0.5 (VG_I). Random selection keeps at most 10 boxes per image, resulting in a reduction of about 50% of the data. Random

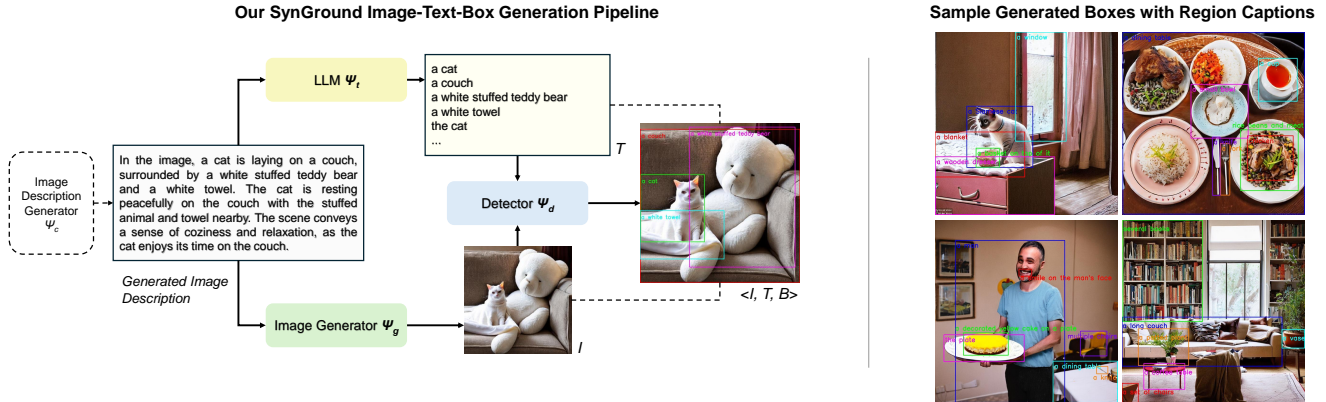


Figure 2. On the left, an overview of our SynGround image-text-box synthesis pipeline, and on the right some sample generated image-text-box triplets. We use an image description generator Ψ_c to output a description that serves as a prompt to an image generator Ψ_g to obtain synthetic image I . This description is also used to obtain text phrases T by prompting an LLM Ψ_t . Finally, the synthetic text and image are fed into an object detector Ψ_d to obtain synthetic boxes B .

text-box synthesized images Syn-R (row 5) outperform the all-text-box conditioned variant (Syn-A, row 3). Also, pairing Syn-R with all text-box data from Real VG (row 4) does not match the effectiveness of either Syn-A with all text-boxes or Syn-R with selected text-boxes, underscoring the importance of image-text-box alignment. Sorting by CLIP text dissimilarity to select at most the top ten inputs (Syn-T, VG_T) marginally improves the random selection. Yet, the most significant improvement stems from selecting as many boxes as possible with an IoU below 0.5. The images (Syn-I) generated with this strategy match the best practice in the GLIP-based pipeline (row 10).

Our results show the potential of using a layout-conditioned generative model for image-text-box synthesis. However, either generating non-overlapping and natural layouts or generating text for visually coherent layouts poses a substantial challenge, limiting the advancement to synthesis without real image-text-box data. Even with layout generation models [32, 36], strong constraints of natural composition and non-overlapping bounding boxes detract from their efficiency and effectiveness compared to the object detector approach.

We use our findings to define **SynGround**, a processing pipeline for generating synthetic image-text-boxes for visual grounding (Table 2, row 10). Fig. 2 shows an overview of the SynGround pipeline along with representative examples of our generated image-text-boxes, including images with specific and recognizable entities (the first image shows “a Siamese cat”), complex scenarios with composite subjects (the second image shows “rice, beans and meat”). The third image shows a synthetic person with unrealistic features, observed in several generated results. This contrasts with improvements on RefCOCO+ Test A (a person-only subset), suggesting that realistic object details are not crucial for visual grounding. The fourth image showcases

creative objects with unusual attributes such as a pink coffee table, which showcases diversity in our generated data. *More qualitative examples are in the supp. materials.*

3.3. Using Real and/or Synthetic Data

SynGround can augment training with real data. Table 3 presents comparisons between training exclusively on real data from the Visual Genome (VG) dataset, synthetic data from SynGround, and a combination of both. The baseline performance (row 1) is significantly enhanced by incorporating synthetic data, yielding an average improvement of 4.81% (row 3). While it falls short of the gains achieved through training on real data (row 2), SynGround offers an average improvement of 9.16% when combined with real data (row 5), outperforming the state-of-the-art (row 2) [94] on RefCOCO+ [97] Test A and B, and Flickr30k [63] benchmarks using Pointing Game accuracy. More importantly, the SynGround generation takes 501 GPU hours on a single NVIDIA A40, which is around 1/9 of VG’s data curation time from 33,000 unique workers [39]. The performance, obtained by training on a percentage of the VG dataset that could plausibly be collected within an equivalent time span using 33,000 human annotators as reported in the original study (row 3), is on par with $SynGround_S$. *Computation details and comparisons are in the Supp.*

4. Implementation Details

Image-Text-Box Synthesis. To favor reproducibility and accessibility, we adopted Stable Diffusion 2.1 [68] with guidance scale 10.0 as the text-to-image generator Ψ_g , an open-source LLM Vicuna-13B [13] as Ψ_t , and GLIP [45] as the object detector Ψ_d . We selected the box with top-1 confidence if it exceeds the default confidence threshold (0.7) in the official implementation. For image description generation Ψ_c , we experimented with BLIP-2 [43] and

Table 3. Training on synthetic and/or real data. We compare visual grounding improvements for the base model (row 1), using the full amount of real data from VG (row 2), a percentage of the real data from VG that could be plausibly annotated by 33,000 human workers in the same time that it takes to generate SynGround images on a single GPU (row 3), synthetic data (row 4), and both (row 5).

Method	Data	#Images	$\langle I, T, B \rangle$	RefCOCO+		Flickr30k	Δ_{avg}
				Test A	Test B		
ALBEF [41]	Off-the-Shelf	–	–	69.35	53.77	79.38	-
AMC [94]	Real	94,893	1,649,546	78.89	61.16	86.46	+8.00
AMC'	Real	76,829	183,282	76.96	59.07	85.01	+6.18
SynGround _S	Synthetic	94,893	998,406	73.70	56.35	86.89	+4.81
SynGround	Real&Synthetic	189,786	2,627,952	79.06	63.67	87.26	+9.16

LLaVA 1.5 [48] for the *Image2Text* strategy. For the *Concept2Text* variant, we used Vicuna-13B [13] to generate image descriptions from a two-concept query with four randomly sampled in-context examples. The concept list contains nouns extracted from real VG captions. The in-context learning example database implementation details are in the *supplementary material*.

Visual Grounding Tuning. The main base model ALBEF-14M [41] is the same as that adopted by the current Sota fully- [94] and weakly-supervised methods [30] for Pointing Game accuracy metric. ALBEF is pretrained on image-text pairs from CC [9], ImageNet-1k [73], MS-COCO [47], SBU Captions [58] and VG [39]. Tuning for visual grounding applies \mathcal{L}_{v1} on image-text pairs and a combination of \mathcal{L}_{v1} and \mathcal{L}_{amc} on image-text-box triplets, adhering to the coefficient settings $\delta_1 = 0.5$, $\delta_2 = 0.1$, $\lambda_1 = 0.8$, and $\lambda_2 = 0.2$ as originally proposed in Yang *et al.* [94]. The training is conducted on a single node with 8 NVIDIA A40 GPUs. Input images are resized to 256×256 pixels and augmented with color jittering, horizontal flipping, and random grayscale conversion. All ALBEF-based experiments use an Adam optimizer [38] with a learning rate set to $1e-5$ and a batch size of 512.

5. Discussion and Analysis

In this section we analyze the effectiveness of SynGround and what are the contributing factors to its performance with respect to real data (Sec 5.1), further validation of SynGround under BLIP (Sec 5.2), effect of dropping dependency on real images entirely (Sec 5.3), performance at various data scales (Sec 5.4), and comparison against web-crawled data (Sec 5.5).

5.1. Real-Synthetic Performance Gap Factors

Table 4 analyzes the factors contributing to the performance gap between synthetic and real data. Experiment I is the off-the-shelf ALBEF performance, serving as a baseline. Experiment II provides the results from training on real

Table 4. Factors causing the performance gap with the real data. We investigate how each model caused the ineffectiveness compared to the real data. ‘R’ for real and ‘S’ for synthetic. I: Off-the-shelf base model. II: Learning from real data. III-V: Sequentially replacing real boxes, text, and images with synthetic variants.

Ex.	Image	Text	Box	$\langle I, T, B \rangle$	RefCOCO+		Flickr30k	Δ_{avg}
					Test A	Test B		
I	-	-	-	-	69.35	53.77	79.38	-
II	R	R	R	1.65M	78.89	61.16	86.46	+8.00
III	R	R	S	1.60M	76.88	59.79	86.76	+6.98
IV	R	S	S	1.00M	73.11	57.35	87.49	+5.15
V	S	S	S	0.99M	73.70	56.35	86.89	+4.81

VG image-text-boxes, leading to an average improvement of 8%. Experiment III retains real images and texts from VG, but employs GLIP-generated boxes. The 1.02% decrease in performance compared to Experiment II suggests that the synthetic boxes, while effective, may lack the precision of manual-annotated equivalents. Experiment IV further replaces real VG captions with synthetic captions from SynGround (*i.e.*, LLaVA_S), resulting in an additional average reduction of 1.83%. This decline could stem from a reduction in the number of captions ($\sim 600K$ fewer) or discrepancies in image-text alignment, coverage, and diversity compared to manually curated captions (*details in the supplementary material*). Interestingly, the performance on Flickr30k is enhanced by 1.03% over real data (II), showing a potential distribution shift from synthetic captions. In Experiment V, the setting consists entirely of synthetic image-text-box data, eliminating real images from the dataset. Compared to Experiment IV, it modestly drops another 0.34%. This minor decrement, relative to the changes observed with synthetic texts and boxes, indicates that synthetic images maintain a level of effectiveness for visual grounding tasks comparable to their real counterparts.

Table 5. Training on both synthetic and real data. We compare grounding improvements for BLIP (I) by using the real data (II, IV) and synthetic data (III, V) w/o the AMC box-supervised loss.

Ex. Box	Data	$\langle I, T, B \rangle$	RefCOCO+		Flickr30k	Δ_{avg}
			Test A	Test B		
I	× Off-the-Shelf	-	58.56	38.00	64.54	-
II	× Real	1.65M	68.86	52.85	64.08	+8.23
III	× Synthetic	0.99M	63.45	44.39	68.21	+4.98
IV	✓ Real	1.65M	78.47	61.96	85.35	+21.56
V	✓ Synthetic	0.99M	71.78	54.82	85.83	+17.11

Table 6. Performance gap between real and synthetic data analyses with BLIP. We investigate how each model caused the ineffectiveness compared to the real data. “R” for real and “S” for synthetic. I: Off-the-shelf. II: Trained on real data. III-V: Sequentially replacing real boxes, text, and images with synthetic variants.

Ex.	Image	Text	Box	$\langle I, T, B \rangle$	RefCOCO+		Flickr30k	Δ_{avg}
					Test A	Test B		
I	-	-	-	-	58.56	38.00	64.54	-
II	R	R	R	1.65M	78.47	61.96	85.35	+21.56
III	R	R	S	1.59M	75.72	58.50	86.11	+19.74
IV	R	S	S	1.00M	72.44	55.94	86.72	+18.00
V	S	S	S	0.99M	71.78	54.82	85.83	+17.11

5.2. Efficacy and Generalization on Other VLMs

This section experiments with an additional off-the-shelf VLM, BLIP [42], to further examine the effectiveness of our synthetic data and verify the generalizability of our findings from the default base model ALBEF. Refer to the supplementary material for the base model selection and implementation details. As shown in Table 5, our generated synthetic image-text and image-text-boxes significantly enhance its visual grounding performance (III, V), matching closely to the improvement from training on real data (II, IV). Additionally, we investigate the factors contributing to the degradation in Table 6. Similar to findings from ALBEF experiments in Sec. 5.1, most drop comes from the box and text synthesis. In supplementary materials, consistent findings are observed by replacing ALBEF with BLIP for experiments presented in previous sections. Moreover, our synthetic data also helps the other type of grounding models [88] that predicts boxes evaluated by Acc@0.5.

5.3. Effect of Less to No Reliance on Real Images

This section explores a series of variants of our methodology that we refer to as SynGround^H, which consists of synthesizing image-text-boxes with less or even no reliance on real data. SynGround^H substitutes real images and the image captioning model with an extracted concept list, an

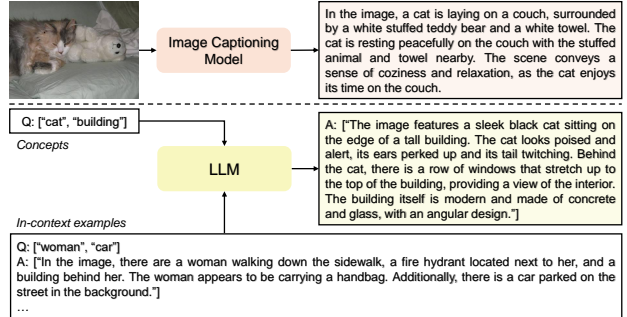


Figure 3. Two approaches for generating image descriptions (Ψ_C) for image synthesis and phrase extraction. The top pipeline, *Image2Text*, relies more on real data, applying an image captioning model to real images. The bottom pipeline, *Context2Text*, samples concepts from a predefined list and uses an LLM with in-context learning to generate image descriptions.

in-context learning example database, and a large language model (LLM). Fig. 3 presents an overview of SynGround^H.

The *Image2Text* strategy, detailed in Sec. 3.2, applies an image captioner to obtain detailed descriptions from real images I^R (II). In contrast, *Context2Text* reduces real data dependency by sampling from a predefined concept list and an in-context learning example database of detailed captions. The concept list is collected from real text T^R , and the in-context learning example database is built through captioning on a small subset of real images I^R (III-V), web-crawled images (VI), or manual-crafted descriptions (VII). Using the in-context learning capability of an LLM Ψ_t , *Context2Text* can theoretically generate unlimited data.

As shown in Table 7, though relying on less or even no real data, the *Context2Text* strategies (SynGround^H) not only rivals but match the performance of the *Image2Text* variant on benchmarks. Sourcing in-context examples (ICE) from captioning on real images, web-crawled data, or manual-crafted text descriptions, while reducing the reliance on real data, all achieve absolute average improvements of around 4%. It indicates the potential of generating synthetic data in a more scalable and flexible setting. More implementation details in the supplementary material.

5.4. Effect of Data Scale on Visual Grounding

This section explores the scalability of synthetic data. We start the image-text-box synthesis at the scale of 250k and then extend it to 1M (SynGround). We sample 3 times from the 1M SynGround data and experiment with each scale to measure variance. Fig. 4 illustrates the average pointing game accuracy improvement across RefCOCO+ [97] and Flickr30k [63]. We plot the mean improvement at each scale with lines and their standard deviations with error bars. The observed upward trend indicates a promising scaling-up ability to use synthetic data with SynGround.

Table 7. Performance comparisons with pipelines at different real data reliance due to different image description generators. SynGround_S (II) relies more on real data, whereas SynGround_S^H (III-VII) reduces reliance through a concept list and in-context examples from different sources.

Ex.	ICE	VG	Img. Source	RefCOCO+		Flickr30k	Δ_{avg}
				Test A	Test B		
I	-	-	-	69.35	53.77	79.38	-
II	-	94,893	Real	73.70	56.35	86.89	+4.81
III	50	50	Real	72.48	56.23	86.07	+4.09
IV	100	100	Real	72.49	56.25	86.33	+4.19
V	500	500	Real	72.18	55.92	86.30	+3.97
VI	500	0	Web	72.69	55.66	86.29	+4.05
VII	500	0	Manual	71.27	56.82	86.78	+4.12

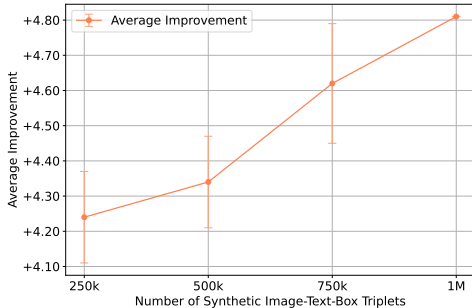


Figure 4. Pointing game accuracy improvement on RefCOCO+ and Flickr30k at various scales. The line denotes the mean improvement across 3 sampled subsets at each scale, and the error bars are corresponding standard deviations.

5.5. Synthetic Data vs. Web-Crawled Data

To showcase the challenge and necessity of generating effective synthetic data tailored for visual grounding, Table 8 compares our synthetic data and web-crawled data. The first and second rows are the off-the-shelf and tuning on real VG data, respectively. For fair comparisons, we randomly sample 1M web-crawled data from Conceptual Captions (CC) [80], approximately matching the scale of our synthetic data. As CC data only encompasses images and texts, we add synthetic boxes using an open-vocabulary detector [45], as the same in our method. Tuning the base model on it achieves (row 3) a 1.82% average performance gain. Additionally, experiments in Table 1 and other work [30] find that visual grounding ability can be enhanced more significantly with object-centric short phrases rather than generic image descriptions. Considering that CC text might describe entire scenarios, we further apply our LLM phrase extraction (row 4) and generate synthetic boxes for the synthetic text phrases, leading to a greater average improvement of 2.86%. However, to our best effort, we can not make the web-crawled data reach a similar enhancement

Table 8. Comparisons of our synthetic data with web-crawled data. The first row is the off-the-shelf base model performance, and the second is the performance after tuning on real data. The third row (“CC”) tunes on a subset of CC [80] image-text pairs with generated synthetic boxes, while “CC_{Phrase}” processes the text through LLM phrase extraction. SynGround_S^H and SynGround_S refer to tuning on our synthetic data, relying less or more on the real data during synthesis, respectively.

Method	Data	$\langle I, T, B \rangle$	RefCOCO+		Flickr30k	Δ_{avg}
			Test A	Test B		
ALBEF [41]	-	-	69.35	53.77	79.38	-
AMC [94]	Real	1,649,546	78.89	61.16	86.46	+8.00
CC	Web	1,000,000	69.05	54.96	83.94	+1.82
CC _{Phrase}	Web	1,000,000	70.35	55.31	85.43	+2.86
SynGround _S ^H	Synthetic	719,254	71.27	56.82	86.78	+4.12
SynGround _S	Synthetic	998,406	73.70	56.35	86.89	+4.81

with our synthetic data (SynGround_S^H, SynGround_S). Our experimental results indicate that it is non-trivial to curate or synthesize image-text-boxes for visual grounding. The image and text favored by visual grounding seem to feature specific properties, such as images with multiple objects and text for region descriptions.

6. Conclusion

This paper investigates various strategies and conducts extensive analyses for generating synthetic training data to improve the visual grounding ability of a base vision-and-language model. By leveraging exhaustive image descriptions for image synthesis, utilizing an LLM for phrase extraction, and adopting an open-vocabulary object detector for box synthesis, we propose SynGround— an effective framework to generate training data for improving visual grounding. SynGround can augment real data to yield further performance gains, and surpasses the efficacy of web-crawled data in visual grounding. Furthermore, SynGround is scalable and capable of generating theoretically infinite data using LLMs for image description generation.

Limitations and Future Work. While SynGround learns from various large-scale pretrained models, it also inherits their limitations, resulting in certain degradations compared to real data. Future improvements could stem from integrating more advanced models, such as GPT-4 [57] or DALLE-3 [5]. Additionally, given the success and efficiency of SynGround, this work has not yet explored the integration of layout-conditioned image synthesis models with less real-data reliance. Although *Context2Image* paradigm can theoretically generate unlimited data, practical limitations in computational resources limit our ability to generate and train on larger-scale data. Future studies should investigate the scaling laws applicable under reduced real data reliance.

References

- [1] Hassan Abu Alhajja, Siva Karthik Mustikovela, Lars Mescheder, Andreas Geiger, and Carsten Rother. Augmented reality meets computer vision: Efficient data generation for urban driving scenes. *International Journal of Computer Vision*, 126:961–972, 2018. 2
- [2] Hassan Akbari, Svebor Karaman, Surabhi Bhargava, Brian Chen, Carl Vondrick, and Shih-Fu Chang. Multi-level multi-modal common semantic space for image-phrase grounding. In *Proceedings of the IEEE/CVF conference on computer vision and pattern recognition*, pages 12476–12486, 2019. 3
- [3] Assaf Arbel, Sivan Doherty, Amit Alfassy, Joseph Shtok, Guy Lev, Eli Schwartz, Hilde Kuehne, Hila Barak Levi, Prasanna Sattigeri, Rameswar Panda, et al. Detector-free weakly supervised grounding by separation. In *Proceedings of the IEEE/CVF International Conference on Computer Vision*, pages 1801–1812, 2021. 2
- [4] Shekoofeh Azizi, Simon Kornblith, Chitwan Saharia, Mohammad Norouzi, and David J Fleet. Synthetic data from diffusion models improves imagenet classification. *arXiv preprint arXiv:2304.08466*, 2023. 1, 2
- [5] James Betker, Gabriel Goh, Li Jing, Tim Brooks, Jianfeng Wang, Linjie Li, Long Ouyang, Juntang Zhuang, Joyce Lee, Yufei Guo, et al. Improving image generation with better captions. *Computer Science*. <https://cdn.openai.com/papers/dall-e-3.pdf>, 2(3):8, 2023. 8
- [6] Nitzan Bitton-Guetta, Yonatan Bitton, Jack Hessel, Ludwig Schmidt, Yuval Elovici, Gabriel Stanovsky, and Roy Schwartz. Breaking common sense: Whoops! a vision-and-language benchmark of synthetic and compositional images. In *Proceedings of the IEEE/CVF International Conference on Computer Vision*, pages 2616–2627, 2023. 1
- [7] Paola Cascante-Bonilla, Hui Wu, Letao Wang, Rogerio S Feris, and Vicente Ordonez. Simvqa: Exploring simulated environments for visual question answering. In *Proceedings of the IEEE/CVF Conference on Computer Vision and Pattern Recognition*, pages 5056–5066, 2022. 2
- [8] Paola Cascante-Bonilla, Khaled Shehadeh, James Seale Smith, Sivan Doherty, Donghyun Kim, Rameswar Panda, Gul Varol, Aude Oliva, Vicente Ordonez, Rogerio Feris, et al. Going beyond nouns with vision & language models using synthetic data. In *Proceedings of the IEEE/CVF International Conference on Computer Vision*, pages 20155–20165, 2023. 2
- [9] Soravit Changpinyo, Piyush Sharma, Nan Ding, and Radu Soricut. Conceptual 12m: Pushing web-scale image-text pre-training to recognize long-tail visual concepts. In *Proceedings of the IEEE/CVF Conference on Computer Vision and Pattern Recognition*, pages 3558–3568, 2021. 2, 6, 1
- [10] Yuhua Chen, Wen Li, Xiaoran Chen, and Luc Van Gool. Learning semantic segmentation from synthetic data: A geometrically guided input-output adaptation approach. In *Proceedings of the IEEE/CVF conference on computer vision and pattern recognition*, pages 1841–1850, 2019. 2
- [11] Yen-Chun Chen, Linjie Li, Licheng Yu, Ahmed El Kholy, Faisal Ahmed, Zhe Gan, Yu Cheng, and Jingjing Liu. Uiter: Universal image-text representation learning. In *European conference on computer vision*, pages 104–120. Springer, 2020. 1, 2
- [12] Zhihong Chen, Ruifei Zhang, Yibing Song, Xiang Wan, and Guanbin Li. Advancing visual grounding with scene knowledge: Benchmark and method. In *Proceedings of the IEEE/CVF Conference on Computer Vision and Pattern Recognition*, pages 15039–15049, 2023. 1
- [13] Wei-Lin Chiang, Zhuohan Li, Zi Lin, Ying Sheng, Zhanghao Wu, Hao Zhang, Lianmin Zheng, Siyuan Zhuang, Yonghao Zhuang, Joseph E. Gonzalez, Ion Stoica, and Eric P. Xing. Vicuna: An open-source chatbot impressing gpt-4 with 90%* chatgpt quality, 2023. 1, 5, 6, 2
- [14] Yabo Dan, Yong Zhao, Xiang Li, Shaobo Li, Ming Hu, and Jianjun Hu. Generative adversarial networks (gan) based efficient sampling of chemical composition space for inverse design of inorganic materials. *npj Computational Materials*, 6(1):84, 2020. 2
- [15] Samyak Datta, Karan Sikka, Anirban Roy, Karuna Ahuja, Devi Parikh, and Ajay Divakaran. Align2ground: Weakly supervised phrase grounding guided by image-caption alignment. In *Proceedings of the IEEE/CVF international conference on computer vision*, pages 2601–2610, 2019. 2, 3
- [16] Celso M de Melo, Antonio Torralba, Leonidas Guibas, James DiCarlo, Rama Chellappa, and Jessica Hodgins. Next-generation deep learning based on simulators and synthetic data. *Trends in cognitive sciences*, 2022. 2
- [17] Chaorui Deng, Qi Wu, Qingyao Wu, Fuyuan Hu, Fan Lyu, and Mingkui Tan. Visual grounding via accumulated attention. In *Proceedings of the IEEE conference on computer vision and pattern recognition*, pages 7746–7755, 2018. 2
- [18] Jiajun Deng, Zhengyuan Yang, Tianlang Chen, Wengang Zhou, and Houqiang Li. Transvg: End-to-end visual grounding with transformers. In *Proceedings of the IEEE/CVF International Conference on Computer Vision*, pages 1769–1779, 2021. 2
- [19] Karan Desai, Gaurav Kaul, Zubin Aysola, and Justin Johnson. Redcaps: Web-curated image-text data created by the people, for the people. *arXiv preprint arXiv:2111.11431*, 2021. 2
- [20] Alexey Dosovitskiy, German Ros, Felipe Codevilla, Antonio Lopez, and Vladlen Koltun. Carla: An open urban driving simulator. In *Conference on robot learning*, pages 1–16. PMLR, 2017. 2
- [21] Zi-Yi Dou and Nanyun Peng. Improving pre-trained vision-and-language embeddings for phrase grounding. In *Proceedings of the 2021 Conference on Empirical Methods in Natural Language Processing*, pages 6362–6371, 2021. 1, 2, 3
- [22] Zi-Yi Dou, Yichong Xu, Zhe Gan, Jianfeng Wang, Shuohang Wang, Lijuan Wang, Chenguang Zhu, Pengchuan Zhang, Lu Yuan, Nanyun Peng, et al. An empirical study of training end-to-end vision-and-language transformers. In *Proceedings of the IEEE/CVF Conference on Computer Vision and Pattern Recognition*, pages 18166–18176, 2022. 2
- [23] Lijie Fan, Kaifeng Chen, Dilip Krishnan, Dina Katabi, Phillip Isola, and Yonglong Tian. Scaling laws of synthetic images for model training... for now. *arXiv preprint arXiv:2312.04567*, 2023. 1, 2

- [24] Chuang Gan, Jeremy Schwartz, Seth Alter, Damian Mrowca, Martin Schrimpf, James Traer, Julian De Freitas, Jonas Kubilius, Abhishek Bhandwaldar, Nick Haber, et al. Threedworld: A platform for interactive multi-modal physical simulation. *arXiv preprint arXiv:2007.04954*, 2020. 2
- [25] Eyal Gomei, Tal Shaharabany, and Lior Wolf. Box-based refinement for weakly supervised and unsupervised localization tasks. In *Proceedings of the IEEE/CVF International Conference on Computer Vision*, pages 16044–16054, 2023. 2
- [26] Klaus Greff, Francois Belletti, Lucas Beyer, Carl Doersch, Yilun Du, Daniel Duckworth, David J Fleet, Dan Gnanaprasam, Florian Golemo, Charles Herrmann, et al. Kubric: A scalable dataset generator. In *Proceedings of the IEEE/CVF Conference on Computer Vision and Pattern Recognition*, pages 3749–3761, 2022. 2
- [27] Tanmay Gupta, Arash Vahdat, Gal Chechik, Xiaodong Yang, Jan Kautz, and Derek Hoiem. Contrastive learning for weakly supervised phrase grounding. In *European Conference on Computer Vision*, pages 752–768. Springer, 2020. 1, 2, 3
- [28] Kaiming He, Georgia Gkioxari, Piotr Dollár, and Ross Girshick. Mask r-cnn. In *Proceedings of the IEEE international conference on computer vision*, pages 2961–2969, 2017. 2
- [29] Ruifei He, Shuyang Sun, Xin Yu, Chuhui Xue, Wenqing Zhang, Philip Torr, Song Bai, and Xiaojuan Qi. Is synthetic data from generative models ready for image recognition? *arXiv preprint arXiv:2210.07574*, 2022. 1, 2
- [30] Ruozhen He, Paola Cascante-Bonilla, Ziyang Yang, Alexander C Berg, and Vicente Ordonez. Improved visual grounding through self-consistent explanations. *arXiv preprint arXiv:2312.04554*, 2023. 2, 3, 6, 8
- [31] Xuanli He, Islam Nassar, Jamie Kiros, Gholamreza Haffari, and Mohammad Norouzi. Generate, annotate, and learn: Nlp with synthetic text. *Transactions of the Association for Computational Linguistics*, 10:826–842, 2022. 2
- [32] Naoto Inoue, Kotaro Kikuchi, Edgar Simo-Serra, Mayu Otani, and Kota Yamaguchi. Layoutdm: Discrete diffusion model for controllable layout generation. In *Proceedings of the IEEE/CVF Conference on Computer Vision and Pattern Recognition*, pages 10167–10176, 2023. 5
- [33] Chao Jia, Yinfei Yang, Ye Xia, Yi-Ting Chen, Zarana Parekh, Hieu Pham, Quoc Le, Yun-Hsuan Sung, Zhen Li, and Tom Duerig. Scaling up visual and vision-language representation learning with noisy text supervision. In *International conference on machine learning*, pages 4904–4916. PMLR, 2021. 1
- [34] Haojun Jiang, Yuanze Lin, Dongchen Han, Shiji Song, and Gao Huang. Pseudo-q: Generating pseudo language queries for visual grounding. In *Proceedings of the IEEE/CVF Conference on Computer Vision and Pattern Recognition*, pages 15513–15523, 2022. 1
- [35] Aishwarya Kamath, Mannat Singh, Yann LeCun, Gabriel Synnaeve, Ishan Misra, and Nicolas Carion. Mdetr-modulated detection for end-to-end multi-modal understanding. In *Proceedings of the IEEE/CVF International Conference on Computer Vision*, pages 1780–1790, 2021. 1, 2
- [36] Kotaro Kikuchi, Edgar Simo-Serra, Mayu Otani, and Kota Yamaguchi. Constrained graphic layout generation via latent optimization. In *Proceedings of the 29th ACM International Conference on Multimedia*, pages 88–96, 2021. 5
- [37] Donghyun Kim, Kaihong Wang, Kate Saenko, Margrit Betke, and Stan Sclaroff. A unified framework for domain adaptive pose estimation. In *European Conference on Computer Vision*, pages 603–620. Springer, 2022. 2
- [38] Diederik P Kingma and Jimmy Ba. Adam: A method for stochastic optimization. *arXiv preprint arXiv:1412.6980*, 2014. 6
- [39] Ranjay Krishna, Yuke Zhu, Oliver Groth, Justin Johnson, Kenji Hata, Joshua Kravitz, Stephanie Chen, Yannis Kalantidis, Li-Jia Li, David A Shamma, et al. Visual genome: Connecting language and vision using crowdsourced dense image annotations. *International journal of computer vision*, 123:32–73, 2017. 1, 2, 5, 6
- [40] Varun Kumar, Ashutosh Choudhary, and Eunah Cho. Data augmentation using pre-trained transformer models. *arXiv preprint arXiv:2003.02245*, 2020. 2
- [41] Junnan Li, Ramprasaath Selvaraju, Akhilesh Gotmare, Shafiq Joty, Caiming Xiong, and Steven Chu Hong Hoi. Align before fuse: Vision and language representation learning with momentum distillation. *Advances in neural information processing systems*, 34:9694–9705, 2021. 1, 2, 3, 4, 6, 8
- [42] Junnan Li, Dongxu Li, Caiming Xiong, and Steven Hoi. Blip: Bootstrapping language-image pre-training for unified vision-language understanding and generation. In *International conference on machine learning*, pages 12888–12900. PMLR, 2022. 7, 2, 4
- [43] Junnan Li, Dongxu Li, Silvio Savarese, and Steven Hoi. Blip-2: Bootstrapping language-image pre-training with frozen image encoders and large language models. *arXiv preprint arXiv:2301.12597*, 2023. 1, 3, 5
- [44] Liunian Harold Li, Mark Yatskar, Da Yin, Cho-Jui Hsieh, and Kai-Wei Chang. Visualbert: A simple and performant baseline for vision and language. *arXiv preprint arXiv:1908.03557*, 2019. 1
- [45] Liunian Harold Li, Pengchuan Zhang, Haotian Zhang, Jianwei Yang, Chunyuan Li, Yiwu Zhong, Lijuan Wang, Lu Yuan, Lei Zhang, Jenq-Neng Hwang, et al. Grounded language-image pre-training. In *Proceedings of the IEEE/CVF Conference on Computer Vision and Pattern Recognition*, pages 10965–10975, 2022. 1, 2, 4, 5, 8
- [46] Yuheng Li, Haotian Liu, Qingyang Wu, Fangzhou Mu, Jianwei Yang, Jianfeng Gao, Chunyuan Li, and Yong Jae Lee. Gligen: Open-set grounded text-to-image generation. In *Proceedings of the IEEE/CVF Conference on Computer Vision and Pattern Recognition*, pages 22511–22521, 2023. 4
- [47] Tsung-Yi Lin, Michael Maire, Serge Belongie, James Hays, Pietro Perona, Deva Ramanan, Piotr Dollár, and C Lawrence Zitnick. Microsoft coco: Common objects in context. In *Computer Vision—ECCV 2014: 13th European Conference, Zurich, Switzerland, September 6–12, 2014, Proceedings, Part V 13*, pages 740–755. Springer, 2014. 6
- [48] Haotian Liu, Chunyuan Li, Qingyang Wu, and Yong Jae Lee.

- Visual instruction tuning. *Advances in neural information processing systems*, 36, 2024. 1, 3, 6
- [49] Jiasen Lu, Dhruv Batra, Devi Parikh, and Stefan Lee. Vilbert: Pretraining task-agnostic visiolinguistic representations for vision-and-language tasks. *Advances in neural information processing systems*, 32, 2019. 1
- [50] Jiasen Lu, Vedanuj Goswami, Marcus Rohrbach, Devi Parikh, and Stefan Lee. 12-in-1: Multi-task vision and language representation learning. In *Proceedings of the IEEE/CVF conference on computer vision and pattern recognition*, pages 10437–10446, 2020. 2, 3
- [51] Zixian Ma, Jerry Hong, Mustafa Omer Gul, Mona Gandhi, Irena Gao, and Ranjay Krishna. Crepe: Can vision-language foundation models reason compositionally? In *Proceedings of the IEEE/CVF Conference on Computer Vision and Pattern Recognition*, pages 10910–10921, 2023. 1
- [52] Yu Meng, Jiaxin Huang, Yu Zhang, and Jiawei Han. Generating training data with language models: Towards zero-shot language understanding. *Advances in Neural Information Processing Systems*, 35:462–477, 2022. 2
- [53] Masato Mimura, Sei Ueno, Hirofumi Inaguma, Shinsuke Sakai, and Tatsuya Kawahara. Leveraging sequence-to-sequence speech synthesis for enhancing acoustic-to-word speech recognition. In *2018 IEEE Spoken Language Technology Workshop (SLT)*, pages 477–484. IEEE, 2018. 2
- [54] Samarth Mishra, Rameswar Panda, Cheng Perng Phoo, Chun-Fu Richard Chen, Leonid Karlinsky, Kate Saenko, Venkatesh Saligrama, and Rogerio S Feris. Task2sim: Towards effective pre-training and transfer from synthetic data. In *Proceedings of the IEEE/CVF Conference on Computer Vision and Pattern Recognition*, pages 9194–9204, 2022. 2
- [55] Arthur Moreau, Nathan Piasco, Dzmitry Tsishkou, Bogdan Stanculescu, and Arnaud de La Fortelle. Lens: Localization enhanced by nerf synthesis. In *Conference on Robot Learning*, pages 1347–1356. PMLR, 2022. 2
- [56] Alex Nichol, Prafulla Dhariwal, Aditya Ramesh, Pranav Shyam, Pamela Mishkin, Bob McGrew, Ilya Sutskever, and Mark Chen. Glide: Towards photorealistic image generation and editing with text-guided diffusion models. *arXiv preprint arXiv:2112.10741*, 2021. 1, 2
- [57] OpenAI. Gpt-4 technical report. *ArXiv*, abs/2303.08774, 2023. 8
- [58] Vicente Ordonez, Girish Kulkarni, and Tamara Berg. Im2text: Describing images using 1 million captioned photographs. *Advances in neural information processing systems*, 24, 2011. 6
- [59] Roni Paiss, Ariel Ephrat, Omer Tov, Shiran Zada, Inbar Mosseri, Michal Irani, and Tali Dekel. Teaching clip to count to ten. In *Proceedings of the IEEE/CVF International Conference on Computer Vision*, pages 3170–3180, 2023. 1
- [60] Xingchao Peng, Baochen Sun, Karim Ali, and Kate Saenko. Learning deep object detectors from 3d models. In *Proceedings of the IEEE international conference on computer vision*, pages 1278–1286, 2015. 2
- [61] Xingchao Peng, Ben Usman, Neela Kaushik, Judy Hoffman, Dequan Wang, and Kate Saenko. Visda: The visual domain adaptation challenge. *arXiv preprint arXiv:1710.06924*, 2017. 2
- [62] Zhiliang Peng, Wenhui Wang, Li Dong, Yaru Hao, Shaohan Huang, Shuming Ma, and Furu Wei. Kosmos-2: Grounding multimodal large language models to the world. *arXiv preprint arXiv:2306.14824*, 2023. 2
- [63] Bryan A Plummer, Liwei Wang, Chris M Cervantes, Juan C Caicedo, Julia Hockenmaier, and Svetlana Lazebnik. Flickr30k entities: Collecting region-to-phrase correspondences for richer image-to-sentence models. In *Proceedings of the IEEE international conference on computer vision*, pages 2641–2649, 2015. 3, 5, 7
- [64] Alec Radford, Jong Wook Kim, Chris Hallacy, Aditya Ramesh, Gabriel Goh, Sandhini Agarwal, Girish Sastry, Amanda Askell, Pamela Mishkin, Jack Clark, et al. Learning transferable visual models from natural language supervision. In *International conference on machine learning*, pages 8748–8763. PMLR, 2021. 1, 2, 4
- [65] Nils Reimers and Iryna Gurevych. Sentence-bert: Sentence embeddings using siamese bert-networks. *arXiv preprint arXiv:1908.10084*, 2019. 3
- [66] Shaoqing Ren, Kaiming He, Ross Girshick, and Jian Sun. Faster r-cnn: Towards real-time object detection with region proposal networks. *Advances in neural information processing systems*, 28, 2015. 2
- [67] Stephan R Richter, Vibhav Vineet, Stefan Roth, and Vladlen Koltun. Playing for data: Ground truth from computer games. In *Computer Vision—ECCV 2016: 14th European Conference, Amsterdam, The Netherlands, October 11–14, 2016, Proceedings, Part II 14*, pages 102–118. Springer, 2016. 2
- [68] Robin Rombach, Andreas Blattmann, Dominik Lorenz, Patrick Esser, and Björn Ommer. High-resolution image synthesis with latent diffusion models. In *Proceedings of the IEEE/CVF conference on computer vision and pattern recognition*, pages 10684–10695, 2022. 1, 5
- [69] German Ros, Laura Sellart, Joanna Materzynska, David Vazquez, and Antonio M Lopez. The synthia dataset: A large collection of synthetic images for semantic segmentation of urban scenes. In *Proceedings of the IEEE conference on computer vision and pattern recognition*, pages 3234–3243, 2016. 2
- [70] Andrew Rosenberg, Yu Zhang, Bhuvana Ramabhadran, Ye Jia, Pedro Moreno, Yonghui Wu, and Zelin Wu. Speech recognition with augmented synthesized speech. In *2019 IEEE automatic speech recognition and understanding workshop (ASRU)*, pages 996–1002. IEEE, 2019. 2
- [71] Nick Rossenbach, Albert Zeyer, Ralf Schlüter, and Hermann Ney. Generating synthetic audio data for attention-based speech recognition systems. In *ICASSP 2020-2020 IEEE International Conference on Acoustics, Speech and Signal Processing (ICASSP)*, pages 7069–7073. IEEE, 2020. 2
- [72] Artem Rozantsev, Vincent Lepetit, and Pascal Fua. On rendering synthetic images for training an object detector. *Computer Vision and Image Understanding*, 137:24–37, 2015. 2
- [73] Olga Russakovsky, Jia Deng, Hao Su, Jonathan Krause, Sanjeev Satheesh, Sean Ma, Zhiheng Huang, Andrej Karpathy, Aditya Khosla, Michael Bernstein, et al. Imagenet large scale visual recognition challenge. *International journal of computer vision*, 115:211–252, 2015. 2, 6

- [74] Chitwan Saharia, William Chan, Saurabh Saxena, Lala Li, Jay Whang, Emily L Denton, Kamyar Ghasemipour, Raphael Gontijo Lopes, Burcu Karagol Ayan, Tim Salimans, et al. Photorealistic text-to-image diffusion models with deep language understanding. *Advances in Neural Information Processing Systems*, 35:36479–36494, 2022. 1, 2
- [75] Mert Bulent Sariyildiz, Karteek Alahari, Diane Larlus, and Yannis Kalantidis. Fake it till you make it: Learning transferable representations from synthetic imagenet clones. In *CVPR 2023–IEEE/CVF Conference on Computer Vision and Pattern Recognition*, 2023. 1
- [76] Christoph Schuhmann, Romain Beaumont, Richard Vencu, Cade Gordon, Ross Wightman, Mehdi Cherti, Theo Coombes, Aarush Katta, Clayton Mullis, Mitchell Wortsman, et al. Laion-5b: An open large-scale dataset for training next generation image-text models. *Advances in Neural Information Processing Systems*, 35:25278–25294, 2022. 1
- [77] Ramprasaath R Selvaraju, Michael Cogswell, Abhishek Das, Ramakrishna Vedantam, Devi Parikh, and Dhruv Batra. Grad-cam: Visual explanations from deep networks via gradient-based localization. In *Proceedings of the IEEE international conference on computer vision*, pages 618–626, 2017. 2, 3
- [78] Tal Shaharabany and Lior Wolf. Similarity maps for self-training weakly-supervised phrase grounding. In *Proceedings of the IEEE/CVF Conference on Computer Vision and Pattern Recognition*, pages 6925–6934, 2023. 2
- [79] Tal Shaharabany, Yoad Tewel, and Lior Wolf. What is where by looking: Weakly-supervised open-world phrase-grounding without text inputs. *Advances in Neural Information Processing Systems*, 35:28222–28237, 2022. 2
- [80] Piyush Sharma, Nan Ding, Sebastian Goodman, and Radu Soricut. Conceptual captions: A cleaned, hypernymed, image alt-text dataset for automatic image captioning. In *Proceedings of the 56th Annual Meeting of the Association for Computational Linguistics (Volume 1: Long Papers)*, pages 2556–2565, 2018. 8
- [81] Yonglong Tian, Lijie Fan, Kaifeng Chen, Dina Katabi, Dilip Krishnan, and Phillip Isola. Learning vision from models rivals learning vision from data. *arXiv preprint arXiv:2312.17742*, 2023. 1, 2
- [82] Yonglong Tian, Lijie Fan, Phillip Isola, Huiwen Chang, and Dilip Krishnan. Stablerep: Synthetic images from text-to-image models make strong visual representation learners. *Advances in Neural Information Processing Systems*, 36, 2024. 1, 2
- [83] Hugo Touvron, Thibaut Lavril, Gautier Izacard, Xavier Martinet, Marie-Anne Lachaux, Timothée Lacroix, Baptiste Rozière, Naman Goyal, Eric Hambro, Faisal Azhar, et al. Llama: Open and efficient foundation language models. *arXiv preprint arXiv:2302.13971*, 2023. 1
- [84] Allan Tucker, Zhenchen Wang, Ylenia Rotalinti, and Puja Myles. Generating high-fidelity synthetic patient data for assessing machine learning healthcare software. *NPJ digital medicine*, 3(1):1–13, 2020. 2
- [85] Gul Varol, Javier Romero, Xavier Martin, Naureen Mahmood, Michael J Black, Ivan Laptev, and Cordelia Schmid. Learning from synthetic humans. In *Proceedings of the IEEE conference on computer vision and pattern recognition*, pages 109–117, 2017. 2
- [86] Gül Varol, Ivan Laptev, Cordelia Schmid, and Andrew Zisserman. Synthetic humans for action recognition from unseen viewpoints. *International Journal of Computer Vision*, 129(7):2264–2287, 2021. 2
- [87] Josiah Wang and Lucia Specia. Phrase localization without paired training examples. In *Proceedings of the IEEE/CVF International Conference on Computer Vision*, pages 4663–4672, 2019. 2
- [88] Peng Wang, An Yang, Rui Men, Junyang Lin, Shuai Bai, Zhikang Li, Jianxin Ma, Chang Zhou, Jingren Zhou, and Hongxia Yang. Ofa: Unifying architectures, tasks, and modalities through a simple sequence-to-sequence learning framework. In *International conference on machine learning*, pages 23318–23340. PMLR, 2022. 7, 3, 4
- [89] Weiyun Wang, Min Shi, Qingyun Li, Wenhui Wang, Zhenhang Huang, Linjie Xing, Zhe Chen, Hao Li, Xizhou Zhu, Zhiguo Cao, et al. The all-seeing project: Towards panoptic visual recognition and understanding of the open world. *arXiv preprint arXiv:2308.01907*, 2023. 2
- [90] Bin Xiao, Haiping Wu, Weijian Xu, Xiyang Dai, Houdong Hu, Yumao Lu, Michael Zeng, Ce Liu, and Lu Yuan. Florence-2: Advancing a unified representation for a variety of vision tasks. *arXiv preprint arXiv:2311.06242*, 2023. 2
- [91] Fanyi Xiao, Leonid Sigal, and Yong Jae Lee. Weakly-supervised visual grounding of phrases with linguistic structures. In *Proceedings of the IEEE Conference on Computer Vision and Pattern Recognition*, pages 5945–5954, 2017. 2
- [92] Li Yang, Yan Xu, Chunfeng Yuan, Wei Liu, Bing Li, and Weiming Hu. Improving visual grounding with visual-linguistic verification and iterative reasoning. In *Proceedings of the IEEE/CVF Conference on Computer Vision and Pattern Recognition*, pages 9499–9508, 2022. 1
- [93] Yiben Yang, Chaitanya Malaviya, Jared Fernandez, Swabha Swayamdipta, Ronan Le Bras, Ji-Ping Wang, Chandra Bhagavatula, Yejin Choi, and Doug Downey. Generative data augmentation for commonsense reasoning. *arXiv preprint arXiv:2004.11546*, 2020. 2
- [94] Ziyang Yang, Kushal Kaffle, Franck Demoncourt, and Vicente Ordonez. Improving visual grounding by encouraging consistent gradient-based explanations. In *Proceedings of the IEEE/CVF Conference on Computer Vision and Pattern Recognition*, pages 19165–19174, 2023. 1, 2, 3, 4, 5, 6, 8
- [95] Lin Yen-Chen, Pete Florence, Jonathan T Barron, Tsung-Yi Lin, Alberto Rodriguez, and Phillip Isola. Nerf-supervision: Learning dense object descriptors from neural radiance fields. In *2022 International Conference on Robotics and Automation (ICRA)*, pages 6496–6503. IEEE, 2022. 2
- [96] Haoxuan You, Haotian Zhang, Zhe Gan, Xianzhi Du, Bowen Zhang, Zirui Wang, Liangliang Cao, Shih-Fu Chang, and Yinfei Yang. Ferret: Refer and ground anything anywhere at any granularity. *arXiv preprint arXiv:2310.07704*, 2023. 2
- [97] Licheng Yu, Patrick Poirson, Shan Yang, Alexander C Berg, and Tamara L Berg. Modeling context in referring expres-

sions. In *Computer Vision–ECCV 2016: 14th European Conference, Amsterdam, The Netherlands, October 11-14, 2016, Proceedings, Part II 14*, pages 69–85. Springer, 2016. [3](#), [5](#), [7](#)

- [98] Jia Zheng, Junfei Zhang, Jing Li, Rui Tang, Shenghua Gao, and Zihan Zhou. Structured3d: A large photo-realistic dataset for structured 3d modeling. In *Computer Vision–ECCV 2020: 16th European Conference, Glasgow, UK, August 23–28, 2020, Proceedings, Part IX 16*, pages 519–535. Springer, 2020. [2](#)

Learning from Synthetic Data for Visual Grounding

Supplementary Material

In this supplementary material, we provide additional implementation details in Section 1, justification of base model selection in Section 2, generalizability of findings in Section 3, efficacy for the box-prediction visual grounding method in Section 4, analyses of synthetic text in Section 5, comparisons between alternative paradigm designs in Section 6, the broader impact in Section 7, and more qualitative examples in Section 8.

1. Implementation Details

This section presents implementation details, including concept list sampling, as well as LLM prompts used for generating image descriptions, summarizing captions, and extracting text phrases.

Q: ["cup", "table"]
A: ["The image showcases a wooden dining table with various food items and tableware arranged on it. A teapot is positioned on the table, along with a kettle and a cup. Three donuts are also present on the table, with one donut placed near the center, another on the left side, and the third on the right side."]

Q: ["couch", "video"]
A: ["In the image, there are two people playing a video game together. A woman is focused on the game, holding a video game remote in her hand, while a man stands behind her, watching her play. There is also a couch in the room, providing a comfortable seating area for the two individuals. Additionally, there is a clock on the wall."]

Q: ["trees", "clock"]
A: ["The image features a tall, multi-story building with a prominent clock tower at the top. The clock is large and can be seen in the center of the tower. The building is surrounded by trees and has a large clock on one of its sides, visible towards the left side of the structure. The overall scene showcases a clock tower that stands out among the surrounding environment."]

Q: ["chair", "vase"]
A: ["The image features a clean, well-furnished apartment with two couches, a chair, and a coffee table. The living room area is bright and open, and a large window allows natural light to fill the space. On the coffee table, there is a vase with a potted plant, and a book is placed on one of the couches."]

Q: ["cars", "trucks"]
A: ["In this scene, a group of people is gathered at a busy street corner with several vehicles, including cars and trucks, surrounding the area. There are multiple police cars parked on the side of the street, as well as other cars and trucks scattered throughout the scene. Two people are holding cell phones, likely communicating with others or checking for updates."]

Figure 5. Random examples from the in-context learning database. The query “Q” contains two nouns, while the expected answer “A” is a crafted image description incorporating the queried nouns.

1.1. Concept2Text: Concept List and In-Context Examples

Following previous work [81], we assume access to a list of concepts and their distribution in real text T^R (captions from the VG dataset [39]). The concept list curation involves tokenizing the real text T^R and identifying nouns by their part-of-speech (POS) tags. To ensure keeping the relevant information provided in a query for image description generation, we exclude a predefined set of nouns commonly used in prompts or spatial positions: “scene”, “scenery”, “view”, “picture”, “image”, “photo”, “left”, “right”, “back”, “front”, “top”, “bottom”, “middle”, “center”, “side”, “background”, “frontmost”, “leftmost”, “rightmost”.

We sample two concepts per query for each image description generation by their frequency in real text T^R . As shown in Fig. 5, an in-context learning example consists of a two-noun query (“Q”) and an image description (“A”).

Q: ["blue metal bike on ground, brown grass fence panel, bicycle parked against the wall, a blue bicycle parked at the railing, a railing of metal pipes and rods, straw fence along the railing, a wood and tan surf board, a tan wood, a red blue and yellow surfboard, a blue and metal bike, an old and rusty bike, a wall, a brown fence panel, a blue surfboard, a surfboard, a white surfboard, a writing, a fence, a boggy board, flame stripes, a brown and boggy board, a blue bicycle, a bicycle, a tan and blue surf board, a railing, a wooden brown and vertical surfboard, metal pipes, a straw fence, a balcony"]
A: ["blue metal old rusty bike, a wooden brown and vertical surfboard, a red blue and yellow surfboard, a tan and blue surfboard, straw fence along the railing, brown and boggy board, flame stripes, balcony, a railing of metal pipes and rods"]

Q: ["this is a person, the cat is black and white, black cat laying on beige carpet, girl playing with cat, fireplace behind the girl, a screen in front of the fireplace, a here person, a here and black cat, a grey and light ground, a girl, a stone fireplace"]
A: ["a girl playing with cat, a black and white cat laying on beige carpet, a grey and light ground, a stone fireplace, a screen in front of the fireplace"]

Q: ["men riding horses on set, two men riding horses on a cobblestone road, two horses have riders but two do not, it is a daytime scene, it is an outdoor scene, there are several people in the photo, there are several horses in the photo, a large brown building, two men on horseback, 2 men and 4 horses, 3 men looking at a motorcycle, 2 men ponying 2 horses, telephone poles on village street, a total of eight people are in this picture, four brown horses with white markings, a man, a horse, some men, some horses, some riders, a daytime, a scene, an outdoor, a sunny, some seems, a sky, some people, a photo, a motorcycle, a motorcycle, some whites, a top, a cowboy, a brown, a cement, a building, a rider, a parked, a street, a road, a horseback, a rocky, a motorbike"]
A: ["two men riding horses on a cobblestone road, four brown horses with white markings, eight people, a large brown building, a motorcycle, telephone poles on village street"]

Q: ["a scene in an old building, a window with green trim, a tan painted brick wall, an a, a window, a top"]
A: ["an old building, a window with green trim, a tan painted brick wall"]

Figure 6. LLM prompts that summarizes real captions in *Text2Text* strategy. Each example comprises a query “Q” in orange and its expected answer “A” in yellow. “Q” is concatenated real text for an image, and “A” is our crafted summary.

Relying less on the real images, the image descriptions are generated by an image captioning model [48] on 50, 100, or 500 randomly sampled real images I^R . In the setting with non-reliance on the real image, we randomly sampled 500 web-crawled images from CC3M [9] or manually crafted 500 text descriptions. Then we use POS to randomly extract two nouns as their query. The *Caption2Text* image de-

Q: ["there are several cars parked on the street, one of which is a red car near the crosswalk"]
A: ["several cars", "the street", "a red car", "the crosswalk"]

Q: ["on the countertop, there is a white plate and a bowl, two cups, a spoon, and a bottle"]
A: ["the countertop", "a white plate", "a bowl", "two cups", "a spoon", "a bottle"]

Q: ["the image features a cluttered home office desk with a variety of objects"]
A: ["a cluttered home office desk", "a variety of objects on the desk"]

Q: ["a computer monitor is situated towards the left side of the desk, accompanied by a keyboard and a mouse placed directly in front of it"]
A: ["a computer monitor", "the left side of the desk", "a keyboard", "a mouse"]

Figure 7. LLM prompts for shorter text phrase T extraction. “Q” is the example query sentence, and “A” is the expected shorter phrase output.

Q: ["there are several cars parked on the street, one of which is a red car near the crosswalk"]
A: ["there are several cars parked on the street", "a red car near the crosswalk"]

Q: ["on the countertop, there is a white plate and a bowl, two cups, a spoon, and a bottle"]
A: ["a white plate on the countertop", "a bowl on the countertop", "two cups on the countertop", "a spoon on the countertop", "a bottle on the countertop"]

Q: ["the image features a cluttered home office desk with a variety of objects"]
A: ["a cluttered home office desk", "a variety of objects on the office desk"]

Q: ["a computer monitor is situated towards the left side of the desk, accompanied by a keyboard and a mouse placed directly in front of it"]
A: ["a computer monitor is situated towards the left side of the desk", "a keyboard and a mouse placed directly in front of the monitor"]

Figure 8. LLM prompts for longer text phrase T extraction. “Q” is the example query sentence, and “A” is the expected longer phrase output.

scription generation uses four random in-context learning examples with a random two-noun query.

1.2. Text2Text: LLM Summary

In the *Text2Text* strategy, we prompt an LLM [13] to condense the potentially redundant VG captions T^R for the same image I^R into a summarized version. We include four examples in our prompts, as detailed in Fig. 6. Note that, for each query “Q” and expected answer “A”, all orange rows correspond to images generated using the captions from the VG dataset (“Q”); as a counterpart, the yellow rows show images generated by the summarized captions (“A”). Compared to directly concatenating all VG captions, the images generated for summary tend to include more salient objects in the prompts (e.g., surfboards in the 2nd row and the girl in the 4th row), enrich the contextual details (e.g., poles in the 6th row), and remain effective for originally concise captions (e.g., the window and wall in the 8th row).

1.3. Image2Text and Concept2Text: Text Phrase Extraction

Unlike image descriptions obtained from *Concatenation* or *Text2Text* strategies, which consist of a list of phrases, the variants in *Image2Text* and *Concept2Text* are expressed as paragraphs. Due to the ineffectiveness of the “period” or “comma” segment (refer to Table 1, main paper), we exper-

imented with partitioning the sentences by phrase extraction through an LLM. We randomly sample four sentences (i.e., segmented by “period”) and extract phrases manually as in-context examples. Fig. 7 presents examples of shorter phrases, while Fig. 8 shows examples of longer phrases.

2. Selection of Base Model

It is non-trivial to select a model that can extensively examine the quality of synthetic data for visual grounding. We select ALBEF [41] as our base model due to its reported off-the-shelf visual grounding performance and success in further improvement with an attention mask consistency objective [94]. Moreover, we intend to generate synthetic data that is effective for both weakly and box-supervised methods, such as the real VG data. The desired model is supposed to be improved with and without box supervision, so that the investigation can be conducted continually and consistently from image-text synthesis to image-text-box synthesis.

To the best of our knowledge, ALBEF is the only VLM fine-tuned with a proposed box-supervised objective (AMC) achieving the current state-of-the-art. Hence, we make our best effort to extract gradient-based explanation maps from other VLMs and implement the AMC loss on top of them. As shown in Table 9, we explore 3 other models, CLIP [64], BLIP [42], and METER [22].

CLIP. We extract the GradCAM [77] attention map from the last layer of the image encoder using its contrastive loss. The weakly-supervised training adopts its contrastive loss. We implement the AMC loss on top of it for box-supervised training. To our best effort, we can not obtain positive results from CLIP by tuning it on the real VG dataset, either weakly or fully. Therefore, CLIP is not a proper choice for visual grounding experiments.

METER. We pick the 5th layer of the cross-modal image encoder and obtain the GradCAM attention map from the image-text matching loss. The weakly-supervised experiments fine-tune METER with its original losses. The box-supervised experiments fine-tune METER with its original losses and an AMC loss we implemented. METER’s original losses are deficient for weakly-supervised tuning. Using the original loss, our best effort for fine-tuning METER on VG significantly decreases performances. When using AMC loss instead, the real data improves METER by 11.24%. Given the deficiency under the weakly-supervised setting, METER can not be easily adopted to investigate both image-text and image-text-boxes continuously.

BLIP. We extract the GradCAM attention maps from the 8th layer of cross-modal attention from image-text match-

Table 9. VLM’s off-the-shelf, weakly-supervised tuned, and AMC box-supervised tuned visual grounding performance in pointing game accuracy.

Model	Box (AMC)	Data	RefCOCO+		Flickr30k	Δ_{avg}
			Test A	Test B		
CLIP	×	Off-the-Shelf	47.42	41.36	59.22	-
	×	VG	44.38	39.09	54.95	-3.19
	✓	VG	33.29	35.71	46.87	-10.71
METER	×	Off-the-Shelf	68.07	52.73	83.16	-
	×	VG	53.44	34.73	57.65	-19.38
	✓	VG	83.16	65.58	88.95	+11.24
BLIP	×	Off-the-Shelf	58.56	38.00	64.54	-
	×	VG	68.86	52.85	64.08	+8.23
	✓	VG	78.47	61.96	85.35	+21.56

ing loss. The weakly-supervised experiments finetune BLIP with its original losses. The box-supervised one fine-tune BLIP with its original losses and an AMC loss we implemented. Training on VG image-text pairs and image-text-box triplets both boosts the grounding performance. Therefore, we select BLIP as an additional model to verify the generalization of our findings.

3. Ablations and Findings with BLIP

Table 10 provides ablation studies with BLIP fine-tuned on synthetic image-text pairs. We observe consistent performance change as ALBEF’s in Table 1, main paper. The Concatenation and Text2Text strategies are ineffective for BLIP as well. In the Image2Text strategy, the shorter phrases extracted from LLaVA captions also fit BLIP better. It is likely due to the nature of visual grounding that focuses on a small RoI (shorter phrases) instead of the entire image or broader RoIs (longer phrases). Also, the longer phrases defined by our prompts contain complex compositions which may affect VLM’s performance. In Table 11, we fine-tune BLIP with image-text-box triplets. Longer phrases (row 3) result in less improvement than the shorter phrases (row 4), which consistently aligns with the findings from ALBEF.

4. Efficacy for the Box-prediction Method

This section shows how our synthetic data helps the visual grounding methods that predict boxes and are evaluated with Accuracy@0.5. We fine-tune the state-of-the-art model in this category, OFA [88], on the real VG data and our synthetic data separately. As shown in Table 12, the second row is the state-of-the-art performance on RefCOCO+, obtained by fine-tuning the pretrained model (row 1) on RefCOCO+ training split. Even though the in-domain training will result in higher results on the corresponding testing set, we posit that the out-of-distribution data is more accessible

and can examine the generalization ability of methods. The off-the-shelf OFA-Base without finetuning on RefCOCO+ (row 1) is much lower than the in-domain (row 2) training-testing result. However, our synthetic data improves OFA dramatically (row 4) and comes close to VG fine-tuning (row 13). Overall, our synthetic data can improve both heatmap-based and box-based grounding methods.

5. Synthetic Text Analysis

This section supplements the analysis of the factors causing the performance gap with the real data in Sec 5.1, main paper. Specifically, here we focus on analyzing the similarity, diversity, and coverage of synthetic text T and real text T^R .

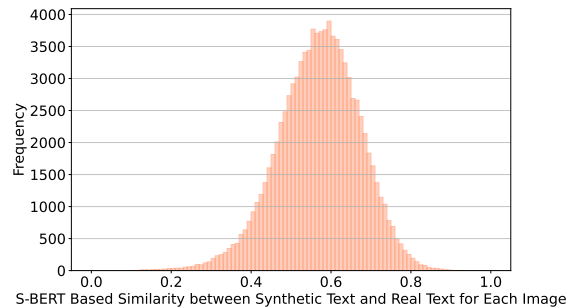


Figure 9. Distribution of image-wise average Sentence-BERT [65] based cosine similarity between synthetic and real text.

To compute the text similarity, we adopt a pretrained Sentence-BERT [65] to encode text into embeddings. Cosine similarity is then calculated between the embeddings of synthetic and real text corresponding to each image. We determine the text similarity for each synthetic caption by selecting the highest similarity among the real text embeddings, and then track the average similarity for each image. The distribution of the average similarity between synthetic

Table 10. Comparisons of image-text synthesis strategies. We assess the effectiveness of synthetic image-text pairs from text concatenation, Text2Text, and Image2Text pipelines by evaluating the performance improvements over a BLIP model Li et al.. For reference we also include the performance that would be obtained by finetuning BLIP on real image-text pairs from Visual Genome (VG).

Category	No.	Image	Text	$\langle I, T, B \rangle$	RefCOCO+		Flickr30k	Δ_{avg}
					Test A	Test B		
BLIP	1	-	-	-	58.56	38.00	64.54	-
BLIP + VG	2	VG	VG	1,649,546	68.86	52.85	64.08	+8.23
Concatenation	3	Syn-C	VG	1,649,546	60.29	41.58	50.98	-2.75
Text2Text	5	Syn-V	LLM _C	530,233	61.79	42.42	55.09	-0.60
Image2Text	6	Syn-L	LLaVA _L	680,093	61.56	42.03	57.69	+0.06
	7	Syn-L	LLaVA _S	1,031,521	63.45	44.39	68.21	+4.98

Table 11. Effectiveness of synthetic image-text-boxes generated with GLIP [45]. For reference we also include the performance that would be obtained by finetuning BLIP [42] with an AMC loss [94] on real image-text-box triplets from Visual Genome (VG).

No.	Image	Text	Box	$\langle I, T, B \rangle$	RefCOCO+		Flickr30k	Δ_{avg}
					Test A	Test B		
1	-	-	-	-	58.56	38.00	64.54	-
2	VG	VG	VG	1,649,546	78.47	61.96	85.35	+21.56
3	Syn-L	LLaVA _L	GLIP	659,927	68.46	54.43	85.73	+15.84
4	Syn-L	LLaVA _S	GLIP	998,406	71.78	54.82	85.83	+17.11

Table 12. Visual grounding performance of OFA-Base [88] on RefCOCO+ in Accuracy@0.5. The first row is the zero-shot performance of the off-the-shelf model. The second row is their reported RefCOCO+ training split fine-tuned performance. The third and fourth rows are VG and SynGround finetuned zero-shot performance, respectively.

Data	RefCOCO+			Δ_{avg}
	Val	Test A	Test B	
-	29.78	31.24	27.82	-
RefCOCO+ [88]	81.39	87.15	74.29	+51.33
VG	54.29	59.52	48.19	+24.39
SynGround	49.53	52.31	45.37	+19.46

and real text for each image is depicted in Fig. 9, where the highest frequency shows a score of around 0.6. The dissimilarity between the synthetic and real text aligns with the observation of degradation from text synthesis compared to real text (Table 4, main paper).

To delve deeper into the distinctions between synthetic and real texts, we compare their text diversity and coverage. Text diversity is measured using the Type-Token Ratio (TTR), which calculates the ratio of unique token types to the total number of tokens in a text. As shown in Fig. 10, our synthetic text T generally has greater diversity than the real text T^R from VG, indicating more elaborate descrip-

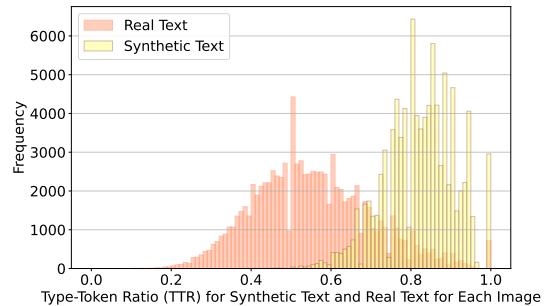


Figure 10. Distribution of image-wise type-token ratio for synthetic and real text.

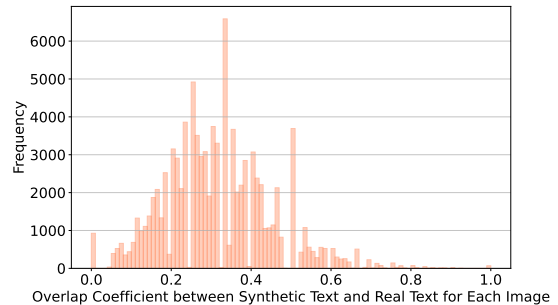


Figure 11. Distribution of image-wise overlap coefficient between synthetic and real text.

Table 13. Data synthesis comparisons. “ReCaption” denotes applying an image captioning model to synthetic images, whereas “Caption” is applied on real images.

Paradigm	RefCOCO+		Flickr30k
	Test A	Test B	
ReCaption	73.09	56.33	86.80
Caption	73.70	56.35	86.89

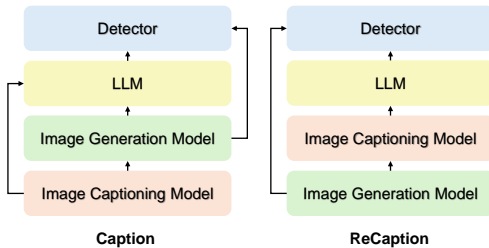


Figure 12. Comparative overview of the “Caption” and “ReCaption” strategies.

tions that, however, may risk including irrelevant words to the visual content. Additionally, we calculate the overlap coefficient between the unique words in synthetic and real text, assessing the coverage and intersection of vocabulary, peaking at around 0.3 (See Fig. 11). This relatively low coefficient reveals the difference in word usage or content focus between the synthetic text T and the real text T^R .

The observation of a higher TTR in synthetic texts T with a modest overlap coefficient with real texts T^R suggests a trade-off for synthesizing more effective texts for visual grounding. Although the broader vocabulary in synthetic texts T suggests richer and more diverse word usage as well as lower repetition when describing an image, the low overlap score implies a divergence from human-annotated content. Moreover, the presence of approximately 600K fewer texts in the synthetic data may indicate that paraphrasing in real data plays a crucial role.

6. Alternative Paradigm Design

Table 13 compares two strategies of distinct sequence on phrase extraction (See Fig. 12). The “Caption” strategy adopted in SynGround obtains the synthetic phrases for visual grounding by applying LLM phrase extraction on captions derived from captioning the real VG images (row 2). Alternatively, “ReCaption” extracts phrases from paragraphs captioned on synthetic images. The core comparison between the “Caption” and “ReCaption” paradigms essentially boils down to evaluating the visual-textual misalignment introduced by image synthesis via a text-to-image model (“Caption”) against the misalignment from an image captioning model (“ReCaption”). Table 13 reveals a

consistent observation with Table 4, main paper, that information loss or misalignment stems from the text synthesis, specifically image captioning on synthetic images in this experiment, rather than the image synthesis.

7. Broader Impact

Using synthetic data for training mitigates privacy issues associated with real images, as the identities of real people are unlikely to be depicted. However, training on synthetic data raises ethical concerns, especially regarding the amplification of implicit biases present in the source data used to train the adopted pretrained models. Such biases may manifest in oversampling specific skin colors and genders, such as in certain caption descriptions.

8. Qualitative Examples

In this section, we supplement additional qualitative examples of our synthetic image-text-boxes. For better display, we randomly present a text phrase if there are multiple phrases for overlapping boxes ($\text{IoU} \geq 0.95$). The full dataset will be released upon publication.

In Fig. 13, the first row showcases indoor scenes, the second row features human-related scenes, and the third row depicts outdoor scenes. Intriguingly, our synthetic data shows diversity, such as unconventional design (e.g., “the lamp”) or color (e.g., “a green chair”, “chairs with a floral pattern”, “red pillows”) of furniture in the first row. Despite the presence of artifacts, synthetic humans generally have human-like shapes (row 2). Considering the experimental results (refer to Table 3, main paper) that tuning on synthetic data improves grounding performance on the RefCOCO+ Test A, a person-only benchmark, the synthetic human with artifacts still benefits visual grounding. The third row presents some challenging scenarios, including small objects (e.g., “traffic lights,” “a train”), detailed descriptions (e.g., “a well-maintained grassy yard”), and complex grammatical structures (e.g., “covered with snow”). In Fig. 14, similar properties are also found in synthetic data generated with less real data reliance (Sec 5.3, main paper). Overall, synthetic data with artifacts is able to improve visual grounding performance based on our result, but we expect learning from more advanced image-generative models or text-generative models can lead to further enhancement.



Figure 13. Qualitative examples of our synthetic image-text-boxes. The images are synthesized by a text-to-image generative model. The texts are generated by an LLM, and their corresponding boxes are obtained from an open-vocabulary object detector.

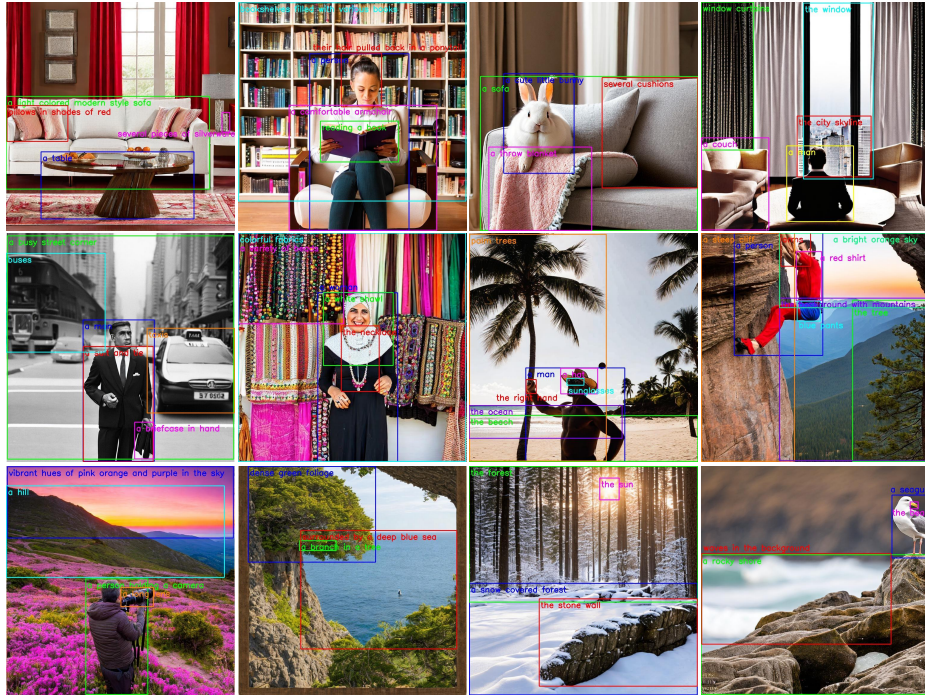


Figure 14. Qualitative examples of our synthetic image-text-boxes generated with *Concept2Text* strategy that relies less on the real data. The images are synthesized according to LLM-generated image descriptions through a text-to-image generative model. The texts are generated by an LLM, and their corresponding boxes are obtained from an open-vocabulary object detector.